Smart Walker Control through the Inference of the User's Command Intentions

M. Martins[1], A. Frizera[2], C. Santos[1] and R. Ceres[3]
[1]*Universidade do Minho, Gualtar, Braga, Portugal*
[2]*Departamento de Engenharia Elétrica, Universidade Federal do Espírito Santo, Vitória, ES, Brazil*
[3]*Grupo de Bioingeniería, Consejo Superior de Investigaciones Científicas,*
Crta Campo Real km 0,200, Arganda del Rey, Madrid, Spain

Keywords: Smart Walker, Assistive Mobility, Fuzzy Control.

Abstract: In this work is presented the NeoASAS walker including its conceptual design, implementation and validation with a new interface approach integrated. This interface is based on a joystick and it is intended to extract the user's movement intentions. Eleven healthy users performed preliminary sets of experiments with the walker, which showed the sensibility of the joystick to extract command intentions from the user. These signals presented a higher frequency component that was attenuated by a Benedict-Bordner filter. Then, an approach to the control architecture was developed, in order to obtain stable and safe user assistance. This control architecture is based on a fuzzy logic control that allows the control of the walkers' motors. Thus, an assistive device to provide safety and natural manoeuvrability was conceived and offers a certain degree of intelligence in assistance and decision-making. The motivation is that this will contribute to improve rehabilitation purposes by promoting ambulatory daily exercises and thus extend users' independent living.

1 INTRODUCTION

Smart walkers are intended to provide increased support and assistance during gait. They are adaptive to their specific application or to the target population and are designed to continually evaluate and correct its actions based on its perception of the users' needs.

In general, Smart walkers have an integrated assistive navigation system and sensors to obstacles detection and there is a concern to allow a stable gait through different handlebar designs (Frizera-Neto, 2010); (Martins, 2011).

In Smart walkers, the user-walker interface is intended to interpret the user's movement intentions and transform this knowledge into motor commands (direction and velocity). This research area has recently witnessed a huge interest in searching for interfaces that can be intuitive and address the fact that users are not required being aware of the intelligent agent behind the driving wheel.

There are many types of interfaces that have been used in smart walkers. Force sensors are the most common, as they can be integrated into handlebars, or in forearm supports (Martins, 2011). In (Frizera-Neto, 2010) despite good results, users may present asymmetries during their gait that lead to different patterns of forces to the same intentions.

These concerns were addressed in (Lee, 2010) by applying infrared sensors to detect the position of lower limbs. However, sensors can mix the legs and therefore make wrong decisions about the users' intentions.

Despite all the advances in the current state-of-the-art user-walker interaction field, there are still many unsolved questions and key areas in determining user-friendly and efficient interfaces. Further, it is very important to remember that these interfaces should not increase the cognitive burden or cause confusion to the lower limb disable users, and should be economic.

Additionally, recent studies on the walker interfaces (Martins, 2011) have not focused on the characterization of the signals gathered by the interface sensors, and it is currently lacking an exhaustive analysis of the main parameters involved in the interface signal. It is required to identify these parameters and their connection to the subsequent

Martins M., Frizera A., Santos C. and Ceres R..
Smart Walker Control through the Inference of the User's Command Intentions.
DOI: 10.5220/0004028704580463
In *Proceedings of the 9th International Conference on Informatics in Control, Automation and Robotics* (ICINCO-2012), pages 458-463
ISBN: 978-989-8565-21-1

algorithms used for detection, recognition and estimation of user's commands.

In this work, it is presented a new interface approach designed to be intuitive and meet usability aspects. The interface integrates a joystick into the walker upper base support. Preliminary studies were conducted with healthy volunteers and no motorization in the device. An analysis of the joystick data was performed and user's navigation commands were identified. These commands are going to be used in the guidance of the walker and recurring to a fuzzy logic strategy, which is fundamental for an efficient control of the device during assistive gait. Then, a validation with the motors on was performed.

This paper is organized as follows. Section II describes the NeoASAS interface constituted by a joystick. Section II also presents and discusses the interaction components acquired with the joystick. Section III discusses the processing strategy to extract the signal components related to the user's navigation commands. Section IV presents and discusses the developed control strategy based on a fuzzy logic system and the achieved results are present in Section V. Finally, conclusions are discussed in Section VI.

2 NeoASAS INTERFACE

The NeoASAS Smart Walker is presented in figure 1. This new robotic walker was built through the mechanical modification of a conventional four-wheeled walker. An additional structure was implemented to integrate the motors and sensors of the robotic walker, as well as forearm supports.

To program all the implemented strategies on the walker, it was used the Matlab and PC/104 platform.

2.1 Specifications of the Novel Interface – Joystick

In this work, the interface consists on placing, at the centre of the upper base support, a joystick associated to a spring that is moved according to user's manipulation (Figure 1). When the user begins his gait, he has to slightly move (less than 1 degree) the handlebar through the handles, moving the joystick, informing the walker which direction and velocity he wants to take. Hence, the user's little efforts are successfully converted into small movements through this new interface.

To extract and study the signals from the joystick, it was performed an user study with 11 healthy volunteers, with no history of any dysfunction on either upper or lower limbs. These volunteers had to perform simple tasks like moving forward and then turn left or right. It is noteworthy that these tests were performed without any motorized system.

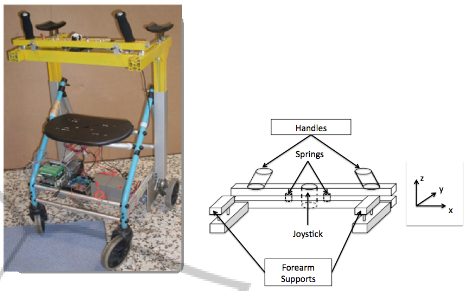

Figure 1: NeoASAS walker and a schematic of the upper base with the joystick.

The joystick outputs three different signals (X,Y,Z), measured in Volts that specify the imposed movement described on the XYZ-axis attached to the joystick. In this work it is just used Y and Z signals.

2.2 Interaction Components

Three types of experiments were performed by the 11 healthy users: walking forward, turn right and turn left (Figure 2). During these two types of signals were acquired and evaluated – forward (Y) and rotation (Z). The Y-signal, gives an indication of the user intention to move forward and according to the applied force on the X-axis, the signal will have more or less amplitude, depending on the user's command intention to go forward with more or less velocity. The Z-signal, gives an indication of the user intention to perform a curve and the signal will present high or low amplitude depending if the performed curve is more or less accentuated. The intention to turn right or left is detected by the sign of the signal, *i.e.* turn left causes negative signal and turn right causes positive signal.

Figure 3 show typical Y and Z joystick data.

Initially, the user is stopped (S1) and both signals are zero. When the user begins to walk forward (S2), he pushes forward the handles of the walker and the Y-signal becomes negative, because the joystick is moved around the X-axis. The Z-signal continues to be zero, since the joystick is not rotated. Sometimes, Z-signal can present some small variations while the user is moving forward. This is associated to users that may present more strength in one arm than in the other.When the user turns right (S3), the joystick is made to move around the Z-axis to the right side also, presenting a negative Z-signal. At the same time, in the Y-axis the joystick tends to go to rest, presenting a zero Y-signal. The next step is to move forward (S4), and the Z-signal returns to zero while the Y-signal becomes negative. At the end of the trajectory, the user stops (S5), and the Y-signal returns to zero. Z-signal remains in zero.

In the case that the user wants to turn right, the only difference is that the Z-signal becomes positive instead negative.

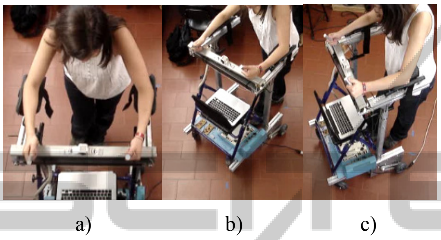

Figure 2: a) Walking forward, b) turning right and c) turning left.

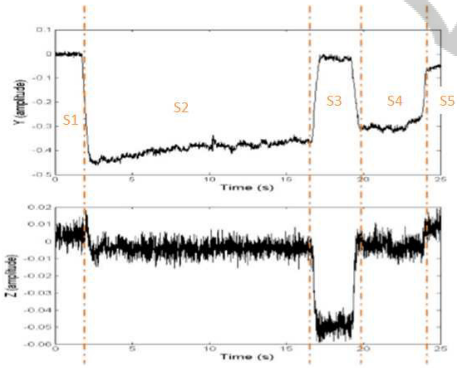

Figure 3: Typical raw Y and Z joystick data in the NeoASAS walker when the user is performing the following trajectory: S1- The user is stopped; S2- User starts walking forward; S3- User turns right; S4- User walks forward; S5 – User stops.

Now, one can conclude that the joystick system read correctly the user's command intentions. However, by observing the characteristics of the signals Z and Y, it can be identified two main components of the signals. One component (i) represents the highest frequency noise caused by the vibrations of the structure. This component must be eliminated in real-time. For that, it will be used a filter which choice will be presented in detail on the next section. The other component (ii) contains the information of the walking movement intentions of the user to guide the walker. This signal will enable the development of robust and secure control strategies.

3 FILTERING STRATEGY

The filtering strategy aims to eliminate in real-time the component (i).

The data that was collected yields that the user's commands intentions occur in a frequency range between 0 and 2 Hz in both Y and Z-signals, and the higher-frequency components are related to noise. In figure 4, one can see the spectrum for typical Y and Z-signals. The Z-signal has more accentuated higher-frequencies than the Y-signal.

The higher frequency components present in the signals can be eliminated with forth and back recursive digital filters, such as Butterworth filters, without causing phase distortion. However, this approach is not real-time implementable. As this technique is not suitable for real-time applications, this filter will be set as a basis to evaluate the performance of the chosen filter strategy.

Besides this, the user should not perceive the delay between his commands and the movement of the walker. The human perception threshold in applications like this is known to be around the 200 ms.

In the literature, two types of filters were identified: g-h filter (Benedict-Bordner and Critically Damped) and the Kalman filter, and they are usually called as tracking filter (E.Brookner, 1998).

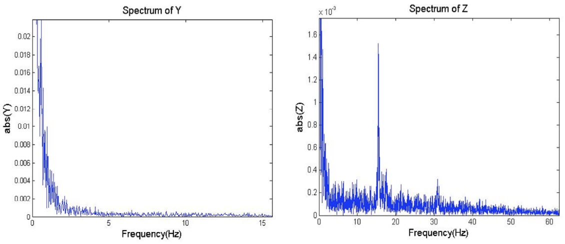

Figure 4: Example of a Frequency Spectrum for (left) raw Y-signal and (right) raw Z-signal.

3.1 User's Movement Intentions Tracking Filters

g-h filter In this filter measurements are used to correct the predictions that are made for the signal, minimizing the estimation error. Formulation is presented in (Brookner, 1998). This filter presents two parameters (*g*,*h*) that need to be offline tuned. To this, the Benedict-Bordner Filter (BBF), equation

(1), and the Critically Damped Filter (CDF), equation (2) will be applied to select the filter parameters.

$$h = \frac{g^2}{2-g} \qquad (1)$$

This equation relates *g* and *h*, such that the BBF has one degree of freedom. In g-h filters increasing the value of *g* diminishes the transient error. Thus, a larger *g* makes the BBF to track higher frequencies.

The (CDF) minimizes the least squares fitting line of previous measurements, giving old data lesser significance when forming the total error sum. This is achieved with a weight factor θ. Parameters in the g–h filter are related by:

$$\begin{aligned} g &= 1-\theta^2 \\ h &= (1-\theta)^2 \end{aligned} \qquad (2)$$

Kalman Filter here depicted is the conventional Kalman filter and is only suitable for linear systems (E.Brookner., 1998).

Therefore, state vector *x(t)* is composed by the variable to be estimated, and its derivative. In the current problem, is considered the system dynamic equations:

$$\begin{aligned} x_{k+1} &= x_k + T\dot{x}_k, \\ \dot{x}_{k+1} &= \dot{x}_k + u_k \end{aligned} \qquad (3)$$

In these equations it is presented a stochastic model that considers a first derivative influenced by a random noise u_k, *i.e.* first derivative is not constant.

The equation that links the actual state x_k and the measured y_k is called the *observation equation:*

$$y_k = x_k + v_k \qquad (4)$$

Where v_k is the process noise.

The Kalman filter parameters will be the measurement noise covariance *R* and the process noise covariance *Q*.

In the implementation of the filter, the measurement noise covariance *R* is measured prior to operation of the filter. Measuring the measurement error covariance *R* is practical because generally it is simple to take some off-line sample measurements in order to determine the average variance of the measurement noise: $R = \left[\sigma_x^2\right]$ Its value is 8.82x10^{-5} rad^2.s^{-2} for the Y-signal noise and 1.3x10^{-5} rad^2.s^{-2} for the Z-signal noise.

The selection of the process noise covariance *Q* is formulated based on the first derivative noise, which affects the estimation of the user's command intentions. The value of *Q* is related to the process error of the system. Thus, a good choice of *Q* helps the filter to estimate more precisely the true state.

It is calculated using of-line measures of the signal. For each measure the covariance of the signal is calculated. Finally, the process noise covariance is the average of all the calculated covariance.

3.2 Evaluation of User's Movement Intentions Trackers Filters

The selection of the BBF parameter *g*, CDF parameter *θ* and Kalman filter parameter *Q*, is presented in this section.

For this selection the Kinematic Estimation Error (KTE) was used. KTE evaluates the smoothness, response time, and execution time of a tracking algorithm (E.Rocón, 2010) and is expressed by:

$$KTE = \sqrt{|\bar{\varepsilon}|^2 + \sigma^2} \qquad (5)$$

$|\bar{\varepsilon}|^2$ and σ^2 are the mean and variance of the absolute estimation error between a desired signal and the measured signal. The desired signal is obtained by filtering offline the signals' measurements with a Butterworth filter.

To select the filters parameters (*g*, *θ* and *Q*), 11 individuals drove the walker without any motorization executing three different trajectories with five repetitions each. During these experiments the signals of the joystick were acquired.

These signals were then introduced off-line in the 3 filters algorithm using a broad range of *g, θ* and *Q* parameters. The result was processed by the KTE. The best solutions for each filter, *i.e.* the ones with the lowest KTE, were chosen for each user, experiment and repetition. With these results, it was calculated the mean of the best 165 solutions for each parameter, as well as the mean of the delay between the input and the output for each case.

Table 1 and 2 present the mean values of the best solutions of *g, θ* and *Q* parameters, delay between the original joystick signal (Y and Z) and the filtered one and KTE for each joystick signal (Y and Z).

Table 1: Filter Parameters based on the KTE and delay for the Y-signal. Table provides for mean±standard deviation.

	Value	KTE (x10^{-3} rad/s)	Delay (ms)
g	44.20±4.97(x10^{-3})	6.46±0.91	0.5±0.25
θ	0.974±3.85x10^{-3}	6.81±0.75	1.7±0.96
Q	3.21±0.55(.10^{-7})	9.66±0.86	17.2±1.86

Table 2: Filter Parameters based on the KTE and delay for the Z-signal. Table provides for mean±standard deviation.

	Value	KTE (x10^{-3} rad/s)	Delay (ms)
g	16.87±2.51(x10^{-3})	2.93±1.99	23.8±1.70
θ	0.990±1.1x10^{-3}	2.99±0.11	25.2±1.59
Q	3.26x10^{-9}±8.78(.10^{-9})	3.12±0.26	36.2±4.00

As it can be seen in Table 1 and 2, *g* of the Z-signal compared with the *g* parameter of the Y-signal shows a lower value. Similarly, the average *θ* and *Q* parameters of the *Z*-signal compared with the average *θ* and *Q* parameters of the *Y*-signal shows a higher value. These results were as expected, since Z-signal required being further filtered.

All filters are of high quality for a human-machine interaction because the introduced delay is much more inferior to human perception (200 ms), not causing prejudice to the human-machine interaction.

KTE is very low for all filters, being the lowest one, the BBF's KTE value, as well as its dispersion. Additionally, the BBF detains the lowest signals' delay.

Since BBF presents the lowest KTE for both signals, one can conclude that it is the best option to choose for this application.

This can also be seen in an example of joystick signal in figure 5, where is presented the differences between BBF and CDF; and figure 6 presents the differences between BBF and Kalman, as well as the reference. The BBF shows a higher attenuation on the oscillations than the CDF and Kalman filters.

Thus, a Benedict-Bordner g-h filter was applied to the joystick data. The g parameter was chosen to be 44.29x10^{-3} for the *Y*-signal and 16.87x10^{-3} for the *Z*-signal. Thus filter has a low computational cost algorithm, making it a good option to this application, since it can run in a low cost hardware with enough robustness for a commercial device.

4 CONTROL STRATEGY

In this section, it is addressed a control strategy based on fuzzy logic to classify the signals sent by the joystick and transform them into motor outputs (direction and velocity), in such way that the walker drives the motors according to the user's commands. The two fuzzy logic inputs will be the Y and Z-signal.

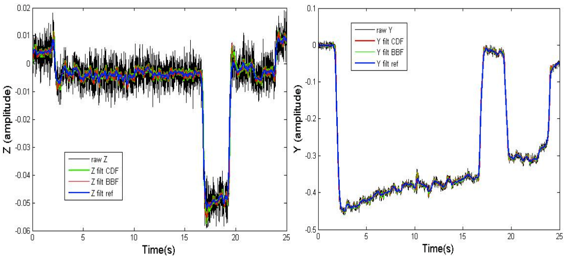

Figure 5: (left) The superposition of the raw Z with the results of BBF, CDF and Butterworth; (Right) The superposition of the raw Y with the results of BBF, CDF and Butterworth.

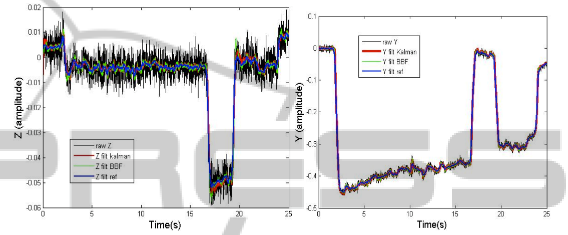

Figure 6: (Left) superposition of the raw Z with the results of BBF, Kalman and Butterworth; (Right) superposition of the raw Y with the results of BBF, Kalman and Butterworth.

It was defined a set of membership functions (MF) for each joystick signal and they were constituted by Gaussian and bell functions. The variables, which form the set of MF for the Z-signal and that will interpret this signal, are divided onto: much left (ME), little left (LE), zero (Zi), little right (LR) and much right (VR). Similarly, the variables, which form the set of MF for the Y-signal and that will interpret this signal, are divided into: negative (Neg), zero (Ze), little positive (PP) and very positive (MP). For the motors right (MR) and left (ML), the output MF set is divided onto: zero (Z), slow (S) and fast (F).The decision-making rules are presented in Table 3.

A series of experiments with motorization were conducted to assess the functioning of the fuzzy system and allow the tuning of the parameters of the implemented system.

Table 3: Decision-making rules. Black (white) columns are related to the left (right) motor.

		Z-signal MF									
		ME		LE		Zi		LR		VR	
Y-signal MF	Neg	Z	S	Z	Z	Z	Z	Z	Z	S	Z
	Ze	Z	F	Z	S	Z	Z	S	Z	F	Z
	PP	S	F	S	F	S	S	F	S	F	S
	MP	S	F	S	F	F	F	F	S	F	S

5 VALIDATION OF THE PURPOSED ARCHITECTURE WITH HEALTHY USERS.

In figure 7, an example of results is shown. The signals were acquired while a user was performing the following trajectory: Start to walk, walk forward, turn left, walk forward and stop. Figure 7 a) shows that with the addition of the motors in the movement of the walker, the Y and Z-signals present a more accentuated noise, comparing with the one saw in figure 3. However, the results from the filter BBF are very satisfactory in attenuating the noise components.

In figure 7 b) it is shown the result obtained before the BBF filter, as well as an adjustment on the gains of the signals. The Y and Z-signal were inverted, amplified and are in the range of [-1,1].

In figure 7 c) the outputs of the fuzzy control system were smoothed and converted to the range of [2.5,5] in order to be sent to the low-level control hardware to command the DC motors.

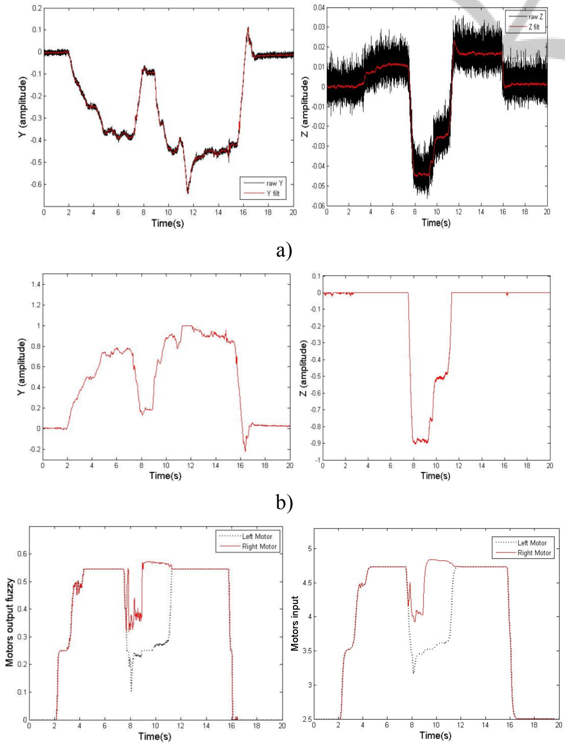

a)

b)

c)

Figure 7: Results from the system architecture of the NeoASAS walker. a) raw acquired joystick signals and the result from the filtering with the BBF filter; b) signals before and after the amplification and restrictions; c) output of the fuzzy system (left) and their integration to then be sent to the control board hardware (right).

Despite the variations of the Y and Z-signal, the motors present a constant and safe movement. Therefore, the system is perfectly adjusted to read the user’s command intentions.

Thus, it was successfully generated a control strategy which has low computational cost, allowing a smooth and enjoyable driving, fast response of the walker and no sense of delay.

6 CONCLUSIONS

In this work it was presented a method of user-walker interaction to extract the users’ command intentions. A series of experiments using with healthy users were performed which showed the sensibility of the joystick to extract navigation commands from the user. The proposed control strategy showed very good results, allowing a smooth and enjoyable driving, fast response of the walker and no sense of delay.

ACKNOWLEDGEMENTS

This work is financiered by FEDER Funds and through *Programa Operacional Fatores de Competitividade* – COMPETE and by National Funds through FCT - *Fundação para a Ciência e Tecnologia* under the Project: FCOMP-01-0124-FEDER-022674.

Work supported by Portuguese Science Foundation (grant SFRH/BD/76097/2011).

REFERENCES

Martins, M., Frizera, A., Santos, C., Ceres, R., (2011). Assistive Mobility Devices focusing on Smart Walkers: Classification and Review. *Robotics and Autonomous Systems*. DOI: 10.1016/j.robot.2011.11.015.

Frizera, A., Gallego, J., Rocon, E., Pons, J., Ceres, R., (2010). Extraction of user’s navigation commands from upper body force interaction in walker assisted gait. *BioMedical Engineering Online*, 9(37), 1-16.

Lee, G., Ohnuma, T., Chong, N., (2010). Design and control of JAIST active robotic walker. *Intel Serv Robotics.*

Brookner, E., (1998). *Tracking and Kalman Filtering Made Easy*. John Wiley & Sons, Inc.

Rocón, E., Ruiz, J., Moreno, J., Pons, J., Miranda, A., (2010). Tremor Characterization: Algorithms for the study of tremor time series. *Sensors.*